TÜBİTAK

Turkish Journal of Earth Sciences

http://journals.tubitak.gov.tr/earth/

Research Article

Turkish J Earth Sci
(2022) 31: 452-466

doi:10.55730/1300-0985.1813

Sedimentary records of trace elements contamination in sediment core from the Gulf of Gemlik, Marmara Sea, Turkey: history, contamination degree, and sources

Tuğçe Nagihan ARSLAN KAYA[1,*], Erol SARI[1], Mehmet Ali KURT[2]
[1]Institute of Marine Science and Management, İstanbul University, İstanbul, Turkey
[2]Department of Environmental Engineering, Mersin University, Mersin, Turkey

Received: 24.05.2022 • **Accepted/Published Online:** 10.08.2022 • **Final Version:** 09.09.2022

Abstract: The pollution history of aluminum (Al), chromium (Cr), cobalt (Co), lead (Pb), zinc (Zn), copper (Cu), and mercury (Hg) were evaluated using geochemical and sedimentological properties of two sediment cores. The MD22A contained a mass-flow unit and two coccolith units. The upper coccolith was characterized by high organic matter, but it was relatively depleted in terms of all studied elements, suggesting dilution by high inorganic carbon. In the mass-flow unit, the relatively high Cr, Co, Zn, and Hg levels suggested additional contamination sources from the Kocadere Stream and Kocasu River. The ranges of Al, Cr, Co, Cu, Hg, Pb, and Zn concentrations in mg kg^{-1} in all core sediment samples were 3510–45840 (Al), 35.7–216.6 (Cr), 3.5–38.1 (Co), 4.5–57.6 (Cu), 17.2–187.2 (Zn), 8.9–71.8 (Pb), and 0.0–0.2 (Hg), respectively. The index of geoaccumulation (I_{geo}), enrichment factor (EF), contamination factor (CF), pollution load index (PLI), and ecological risk index (RI) were used to assess the contamination statuses of the samples. The MD22A core sediments contained more enriched trace elements than the MD89A core sediments. According to EF and I_{geo}, the sediments had moderate enrichment with Cr, Cu, Co, Pb, and Zn and were moderately contaminated with Cr, Co, Zn, Pb, and Hg. RI showed a moderate to high potential ecological risk for the presence of trace elements in the study area. The principal component analysis (PCA) results strongly suggested that the pollution (Cr, Co, Cu, Zn, Pb, and Hg) was mainly caused by anthropogenic activities around the region and transported to the eastern and southern coast of the gulf by the Kocasu River and the Karsak Creek. The upper part of the core in the Gulf of Gemlik has been significantly polluted with Cr, Co, Hg, and Zn since 1930.

Key words: Gulf of Gemlik, trace element, core sediment, sediment quality, principal component analysis

1. Introduction

Trace element pollution in aquatic ecosystems is highly worrying due to these elements' toxicity, bioaccumulation, and persistence properties and adverse effects on human health through the food chain (Bakak et al., 2020; Yu et al., 2021). In recent years, trace elements entered marine environments through lithogenic or anthropogenic pathways, mainly by soil erosion, industrial activities, mining and smelting, agriculture, and urban sewage (Yu et al., 2021). Sediment is one of the major factors of the storage ecosystem (Zhang et al., 2021); it has sensitive indicators for monitoring pollutants in aquatic environments (Vrhovnik et al., 2013; Zhang et al., 2014). When metals enter aquatic environments, they primarily accumulate in fine fragments and suspended particulate substances as a result of interactions such as adsorption, coprecipitation, or metal-ligand bonds (e.g., organic matter, oxides, sulfides, Singh et al., 2017) before getting deposited in marine bottom sediments. The priority pollutants listed by the US Environmental Protection Agency (U.S. EPA, 1986) in aquatic environments are cadmium (Cd), chromium (Cr), copper (Cu), mercury (Hg), lead (Pb), and zinc (Zn), which have been transported and deposited in marine sediments as a result of anthropogenic activities over the last 200 years. Core studies in geochemistry, paleontology, and paleomagnetic are highly valuable and can provide useful information about past environmental conditions (Kırcı Elmas et al., 2007; Sarı et al., 2018; Makaroğlu, 2021). They can also represent historical records of anthropogenic or natural heavy metal accumulations and trace elements based on background reference data over time periods. For this purpose, many researchers have paid importance to these studies (i.e. Kükrer et al., 2019; Varol et al., 2020; Marziali et al., 2021; Young et al., 2021). Although many surface sediment studies have been carried out in the Gulf of Gemlik and Marmara Sea, these studies have generally focused on biodiversity (Taviani et al., 2014; Balcı et al., 2017) and anthropogenic pollution (Algan et al., 2004; Ünlü et al., 2006; Sarı et al., 2013; 2020; Arslan Kaya et al., 2020). There is almost no information available in the

* Correspondence: tugce.arslan@istanbul.edu.tr

literature for trace element pollution in core sediments of the Gulf of Gemlik.

The main aim of this study is to evaluate the pollution history and sediment quality in the Gulf of Gemlik, which may become a baseline for further monitoring research. Therefore, the paper attempts to measure the total organic carbon (TOC), total inorganic carbon (TIC), grain size content, and geochemical concentration of Al, Cr, Co, Cu, Zn, Pb, and Hg elements.

1.1. Description of the study area

The Gulf of Gemlik is a polluted area in the Marmara Sea with high anthropogenic pressure due to riverine inputs, urbanization, coastal shipping, and industrial activities (Ünlü et al., 2008). The gulf was formed as a pull-apart basin during the late Pliocene–early Pleistocene mainly controlled by west-trending dextral strike-slip faults along the middle strand of the North Anatolian Fault Zone (Barka and Kadinsky-Cade, 1988; Barka and Kuşcu, 1996; Yaltırak and Alpar 2002; Yaltırak et al., 2005).

The Gulf of Gemlik is situated in the south-eastern part of the Marmara Sea that comprises a two-layer water structure. The upper layer is of the Black Sea origin (22–26 ppt), the lower layer is of Mediterranean origin (38.5 ppt). These water layers are separated by a sharp pycnocline at –25 m (Beşiktepe et al., 1994). The gulf is a semienclosed basin, with a maximum depth of 113 m, length of 36 km, and width of 11 km (Yaltırak and Alpar, 2002; Vardar et al., 2014). The main sources of fresh water and sediments entering the gulf are the Kocasu River, the Karsak Creek, and the Yaman Creek. The Kocasu River drainage area is 27,600 km², its main branch length is 321 km, and it has an area of 50.7 km² (Özşahin, 2015). The shore length of the Kocasu Delta is 20.8 km; its slope is 1.1‰, and its progression amount is 3.5 km. Its total area that does not contain water is 48 km² (Kazancı et al., 1997; 1999). The Simav, Orhaneli, Mustafakemalpaşa, and Nilüfer branches and Kocaçay are the main tributaries of the Kocasu River (Kazancı et al., 1999). The Kocasu River (flow rate: 171 m³/s; suspended solids: 614,000 t/year; Ergin et al., 1991) carries a significant pollution load from industrial and agricultural areas to the Gulf of Gemlik (Sarı et al., 2008). The Karsak Creek is connected to Lake İznik to the east, whereas there are two big towns around it, and various industrial wastewater and domestic sewerage flow into this channel (Ünlü et al., 2008).

The main anthropogenic sources of pollutants in the region include shipping, domestic discharges from 225,000 inhabitants around the gulf (Gemlik and Mudanya districts), and industrial wastewater discharges, and the area hosts almost 40 industrial plants located in the eastern and southern parts of the gulf, such as tanneries, fertilizer, oil, gas, paint production, and chemical industries, food, textile, and metal industries (Ünlü et al., 2008).

2. Materials and methods

2.1. Sample collection and analysis

The studied cores MD22A (40°22′54.56″K, 28°51′1.79″D) and MD89A (40°25′48.00″K, 29°8′13.79″D) were recovered from the Gulf of Gemlik by using a gravity corer during cruise onboard R/V Alemdar in July 2014 (Figure 1). We assumed that both stations were more polluted areas in the Gulf of Gemlik. The Kocasu River is the most important sediment source in the south, while the Karsak Creek is the most important pollution source in the east. Many industrial complexes use these rivers and discharge their load directly into the Gulf of Gemlik. Both cores were taken from near these river's paleo delta and channels (Figure 1). Afterward, the cores were transported to İstanbul University Institute of Marine Sciences and Management, Marine Geology laboratory. To prevent the sediment cores from deteriorating, we kept them at +4 °C in the core repository until they were described and sampled. Care was taken to protect the sediment samples from contamination during sampling, transportation, and preparation for analysis. The cores were split in two halves, photographed, sampled, and described according of their texture. After the lithological description carried out on split halves, the cores were logged for magnetic susceptibility (MS) and gamma density (GD) at 0.5-cm resolution using a Bartington point sensor mounted on a Geotek Multi-Sensor Core Logger (MSCL) at ITU-EMCOL. One of half was sampled for grain size analysis with 2-cm slices through the core. Another half was sampled for geochemical analysis with 1 cm slices for the top 30 cm below sea floor (cmbsf), 2-cm slices for the 30–60 cmbsf, and 5-cm slices for the 60–100 cmbsf part of the core. The rest of the core was sampled with 10-cm slices. The samples were dried in an oven at 45 °C for 48 h and ground using a mortar and a pestle. The homogenized samples were then stored in labeled glasses until geochemical analysis was performed. Metal analyses were performed using ICP-MS (Agilent 7500 Tokyo, Japan) after total digestion process. For the analysis, approximately 0.2 g of sample was totally digested in a hot HNO3-HF-HClO4-HCl acid mixture using a MARS 240/50 microwave digestion system (CEM, USA). Montana soil (NIST SRM 2710) was used for checking accuracy. Five replicate analyses of reference samples showed good precision, with recovery rates of 92%–102% for the studied elements (Table 1). Total mercury (THg) content was analyzed using Milestone DMA 80. For this analysis, the procedure required samples with a dry weight of approximately 0.25 g. The sample was placed inside a glass tube and then the calculation was done automatically based on 3 times the standard deviation of blank measurements. Replicated analysis (n = 3) of NIST SRM 2976 showed good accuracy (Table 1). Total organic carbon (TOC) analysis was carried out using

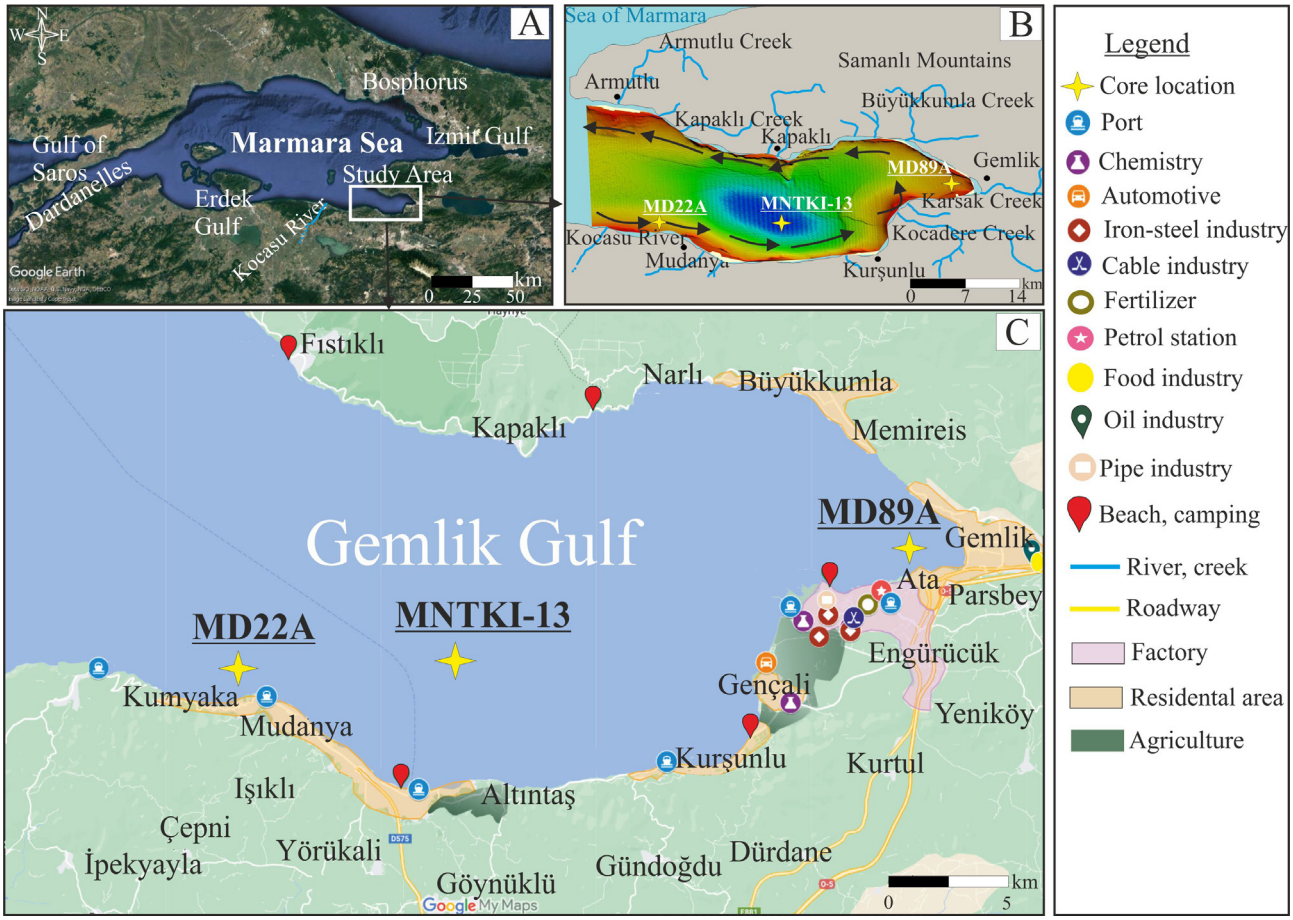

Figure 1. Google Earth map showing locations of (A) Marmara Sea and study area, (B) bathymetry of the Gulf of Gemlik showing the core locations. The gulf is fed by numerous rivers. Black eddies show counterclockwise bottom currents that are mainly derived from the Mediterranean waters (Beşiktepe et al., 1994), and (C) land use map showing main industrial complexes and residential areas around the Gulf of Gemlik.

Table 1. Summary of measured and certified values for Cr, Cu, Co, Zn, and Pb in standard SRM 2710 (mg kg^{-1}) and Hg in standard SRM 2976 (μg kg^{-1}) with five and three replicate analyses, respectively.

Element	Measured value	Certified value	Recovery (%)
Cr	35.63 ± 0.45	39.00[a]	92
Cu	2807.33 ± 26.85	2950.00 ± 130	100
Co	8.96 ± 0.05	10.00[a]	90
Zn	7180.16 ± 27.15	6952.00 ± 91	102
Pb	5067.00 ± 87.16	5532.00 ± 80	95
Hg	63.2 ± 0.7	61.0 ± 3.6	100

[a]Noncertified value

the Walkley Black method. The analysis is based on the titration with ferrous ammonium sulfate of the dichromate left after a wet combustion of the sample with potassium dichromate (Gaudette, 1974; Loring and Rantala, 1992). Total inorganic carbon (TIC) content was determined with a gasometric method (Loring and Rantala, 1992). For this analysis, dry ground sediment was acidified with 10% HCl, followed by volumetric determination of released

CO_2. The TIC contents were converted to weight % total carbonate (i.e. equivalent $CaCO_3$) and expressed as such throughout this paper. Grain size analysis was performed using Micromeritics SediGraph 5120 for mud contents. Gravel (>2 mm) and sand (0.063–2 mm) fractions were analyzed using standard sieves. Grain-size results were combined into three main size fractions: clay (<4 μm), silt (4–63 μm), and sand (63 μm to 2 mm).

2.2. Chronology

Accelerated mass spectroscopy (AMS) radiocarbon dating was carried out at the Marmara Research Center (MAM), TÜBİTAK in Turkey. The unbroken shell was used for radiocarbon analysis. The shells were carefully cleaned, and then inspected under a microscope to ensure that they were diagenetically unaltered. For core MD89A, we used the Calib7.0 software, adopting the IntCal 13.14c Calibration curve of Reimer et al. (2013) to calibrate the age (Table 2). However, we could not construct an age-depth model due to insufficient radiocarbon dates through the core. Therefore, we calculated sedimentation rates for MD89A based on assumption of a uniform sedimentation rate. Our radiocarbon date is reported as measurements without the modern ca. 415-year reservoir correction (Siani et al., 2000). The chronology of core MD22A was established by stratigraphic correlation with core MNTKI-13 from the same basin, which was dated by Albut (2014) using radionuclide method. Both cores show similar sedimentological characteristics, magnetic susceptibility, and gamma density profiles, and include correlatable mass-flow and coccolith units (Figures 2 and 3; see Section 4.2). Radionuclide ages in MNTKI-13 were used to integrate the chronological information for core MD22A (Figure 3; see Section 3.2).

2.3. Assessment of sediment quality

2.3.1. Enrichment factor (EF)

Enrichment factor (EF) was calculated to identify the pollution levels of trace elements (Sutherland, 2000). It can be possible to evaluate the anthropogenic influences on trace elements in sediment from EF (Selvaraj et al., 2004; Duman et al., 2022; Özkan et al., 2022). Anthropogenic influences on trace elements in sediment were evaluated from EF. Al, Fe, Mn, and Rb are widely used as conservative soil elements (Ackerman, 1980; Loring, 1990; Loring and Rantala, 1992). In this study, we used Al because it is a conservative and major element of clay minerals, and has been previously used by several researchers (e.g., Balls et al., 1997; Pekey, 2006). Enrichment factor was calculated using the following equation according to Sutherland (2000):

$$EF = \left(\frac{CM}{CAl}\right) sample / \left(\frac{CM}{CAl}\right) background$$

where (CM/CAl) sediment is the ratio of concentration of the heavy metal to Al concentration (mg kg^{-1}). (CM/CAl) background is the ratio of unpolluted reference value. The EF was categorized into five groups: EF ≤ 2, indicating minor enrichment, 2 < EF < 5 moderate enrichment, 5 < EF < 20 severe enrichment, 20 < EF < 40 very severe enrichment, and EF > 40 extremely severe enrichment (Sutherland, 2000).

2.3.2. Index of geoaccumulation (I_{geo})

I_{geo} was introduced by Muller (1969) to determine metal contamination. I_{geo} was calculated using the following formula:

$$Igeo = Log2\ (\frac{Cn}{1.5(Bn)})$$

where Cn is concentration of the examined metal in the sediment, Bn is background value for the metal n (Turekian and Wedepohl, 1961), and the factor 1.5 is used because of possible variations of the background data due to lithological variations (Usese et al., 2017). According to I_{geo} value, the pollution level of any metal is ranged from class 0 (unpolluted, $I_{geo} < 0$) to class 6 (extremely polluted, $I_{geo} > 5$).

2.3.3. Contamination factor (CF) and pollution load index (PLI)

In this study, pollution degree of trace elements and possible anthropogenic impact on core sediments from the Gemlik Gulf was evaluated using contamination factor (CF) and pollution load index (PLI). The contamination factor of the studied trace elements was calculated with the following equation:

$CF = Cmetal/Cbackground$

Cmetal represents the pollutant concentration in the sediment and Cbackground refers to metal background values. CF values were interpreted as the levels of metal pollution categorized by Sarı et al. (2020); CF < 2 indicating

Table 2. Radiocarbon age obtained for core MD89A. The age is calibrated by using CALIB program. cmbsf; meters below sea floor.

Water depth (m), dated material (lab. number)	Core location	Core depth (cmbsf)	Radiocarbon ages (AD)	Calibrated radiocarbon age (AD)
–38 m, shell (0799)	MD89A	0.58	1216 ± 26	1687 ± 153

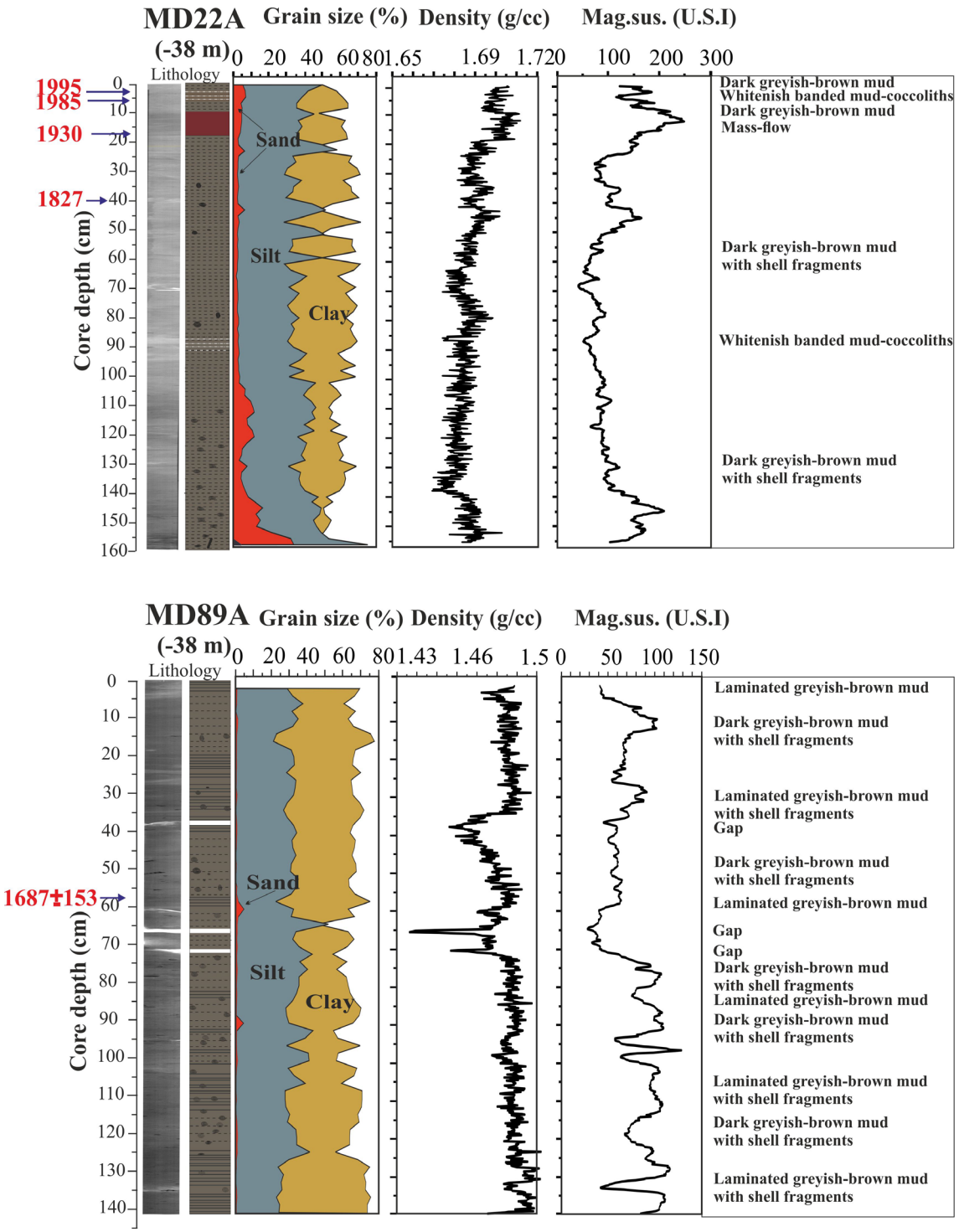

Figure 2. Physical properties (lithological description, grain size, gamma density, and magnetic susceptibility) of cores.

uncontaminated to slightly contaminated sediments, 2 < CF < 4: moderately contaminated sediments, 4 < CF < 6: significantly contaminated sediments, and CF > 6: very highly contaminated sediments.

Pollution load index (PLI) is a useful geostatistical parameter to determine the degree of contamination originating from natural materials or human activities in the marine sediments and has been widely applied by many

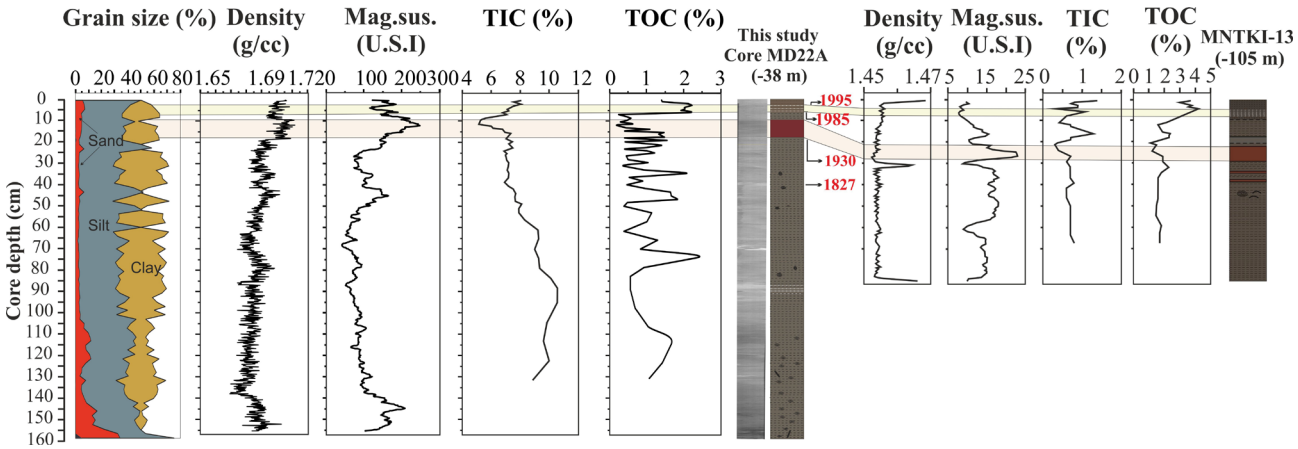

Figure 3. Stratigraphic correlation of cores MD22A and MNTKI-13, based on lithology, magnetic susceptibility, density, and grain size. The lithologic log and radionuclide ages of core MNTKI-13 are from Albut, 2014.

researchers (Bhuiyan et al., 2010; Varol et al., 2022). The PLI is calculated using the following formula (Tomlinson et al., 1980):

$$PLI = \sqrt[n]{(CF1 * CF2 * \ldots CFn)}$$

The PLI values were interpreted as suggested by Tomlinson et al. (1980), where the value of PLI ≤ 1 indicates no pollution, 1 < PLI ≤ 2 is moderate pollution, 2 < PLI ≤ 3 is heavy pollution, and PLI > 3 is extremely heavy pollution.

2.3.4. Ecological risk index (E_r^i) and potential ecological risk index (RI)

Ecological risk E_r^i was created by Swedish scientist Hakanson (1980) to assess the quantitative potential risk of each metal in the sediment to the aquatic ecosystem. E_r^i is calculated using the following equation:

$$E_r^i = Tr * CF$$

$$RI = \sum_{1}^{n} E_r^i$$

RI represents the summing up of all risk factors for trace metals in sediments. (E_r^i) represents the environmental risk index suggested by Hakanson (1980). Tr is the toxic response factor projected by Hakanson (1980) for six metals Zn: 1, Cr: 2, Cu and Pb: 5, As: 10 and Cd: 30, and CF is the contamination factor calculated using the Equal. E_r^i and RI are divided into 5 and 4 categories, respectively. These are E_r^i < 20, RI < 30: low risk; 20 < E_r^i < 40, 30 < RI < 60: moderate risk; 40 < E_r^i < 80, 60 < RI < 120: significant risk; 80 < E_r^i < 160, RI > 120: high risk; E_r^i > 160: very high risk.

2.3.5. Statistical analysis

Multivariate statistics were used to evaluate the characteristics of trace element content in sediment (Rani et al., 2021; Cüce et al., 2022). In this study, PCA and Pearson's correlation coefficient were applied to understand the probable origins of contaminants. The correlation coefficient analysis is a method used to measure the correlativity between heavy metals (Tume et al., 2011, Yang et al., 2011). PCA was examined by the Varimax normalized rotation, Kaiser–Meyer–Olkin (KMO) value (>0.5) and Bartlett sphericity tests ($p < 0.001$) to establish the validity of the data. All statistical analyses were performed in SPSS statistics 21.

3. Results

3.1. Core description and physical properties

The core MD22A consisted of greyish-brown homogeneous mud, locally containing whole and fragmented bivalves, as observed both visually and in the radiographic images (Figure 2). On average, the sediments consisted of 6% sand, 54% silt, and 40% clay (Figure 2). Based on the petrographic examination, most of the coarse fraction in the interval from 100 to 157 cmbsf of this core consisted of calcareous shells and shell fragments. The hemipelagic sedimentary sequence was interrupted by a mass-flow unit that was characterized by a reddish sand-silt-rich basal unit and was probably sourced from the Kocadere Delta front on the eastern shoreline of the Gulf of Gemlik (Gasperini et al., 2011; Taviani et al., 2014; Çağatay et al., 2015) (Figures 2 and 3). The mass-flow unit was easily distinguished from normal hemipelagic sediments by its high gamma and radiographic densities (Figure 3). This unit constituted the upper 10–18 cmbsf interval of the core MD22A and consisted of reddish sandy-silty clay with up

to 5% sand and 45% silt contents. The coarse basal parts of the mass-flow were characterized by a high gamma density and magnetic susceptibility (MS), with maximum values of 1.71 g/cm^3 and 250 u.S.I., respectively (Figure 3). In comparison, the density and MS of the background hemipelagic sediments were relatively low, except for a sharp increase near the core bottom, due to detrital inputs from the Kocasu River. The light laminae in the core sequences were mainly composed of coccoliths. The silt- and sand-sized material mainly consisted of bivalve shell fragments. The intervals of 2.5–7.5 and 86–94 cmbsf were whitish banded mud, and they represented the coccolith units (Figures 2 and 3; see Section 4.2).

The core MD89A consisted of homogeneous greyish-brown mud with microlaminated bands. The concentrations of sand in the core varied between 0.1% and 4% and averaged at 1% (Figure 2). The core sequence was mainly composed of silt and clay that represented many macro- and microfossils. On average, the sediments consisted of 33% silt and 66% clay. The whole core was characterized by a uniform gamma density, ranging from 1.47 to 1.5 g/cm^3. However, from 70 to 90 cmbsf and from 120 to 145 cmbsf, the gamma density dropped sharply with fluctuations between 1.43 and 1.47 g/cm^3 due to the absence of sediments (Figure 2).

3.2. Chronology of cores MD22A and MD89A

As explained in Section 2.2., the chronology of the core MD22A was based on its correlation with the core MNTKI-13 that was recovered from the same basin. MNTKI-13 has been extensively studied and dated by Albut (2014) (Figure 3). Since we can robustly correlate the cores MD22A and MNTKI-13 based on lithology, we used the ages of the mass-flow and coccolith in the core MNTKI-13 for the chronology of the core MD22A. On the basis of radionuclide chronologies, the upper coccolith unit was deposited between 1995 and 1985. The radionuclide analysis of the mass-flow unit revealed an age of 1930. Assuming uniform sedimentation rates after the mass-flow unit (4.6 cm/year), the level at which pollution started (40 cmbsf) corresponded to 1827 (see Section 4.2). The chronology for the core MD89A was based on extrapolation from the radiocarbon age at 58 cmbsf. Based on this assumption, the sedimentation rate was 5.6 cm/year for the core MD89A.

3.3. Trace elements, total organic carbon, and carbonate contents

The vertical distribution patterns for Cr, Co, Cu, Hg, Pb, and Zn in the cores MD22A and MD89A are shown in Figure 4. The ranges of Al, Cr, Co, Cu, Hg, Pb, and Zn concentrations in mg kg^{-1} in all core sediment samples were 3510–45840 (Al), 35.7–216.6 (Cr), 3.5–38.1 (Co), 4.5–57.6 (Cu), 17.2–187.2 (Zn), 8.9–71.8 (Pb), and 0.0–0.2 (Hg). The mean values of the trace element concentrations followed this order: Al (20605) > Cr (139.7) > Zn (95.2) > Cu (40) > Pb (37.3) > Co (24.4) > Hg (0.1) for MD22 and Al (19804) > Cr (99.1) > Zn (71.2) > Cu (37.4) > Pb (24.8) > Co (21.2) > Hg (0.1) for MD89A in mg kg^{-1}.

The mean TIC contents as dry weight % CaCO3 were 7.6 for MD22A and 6.1 for MD89A (Figure 4). The mean and range (in parentheses) values of the TOC contents of the cores MD22A and MD89A were 1.1% (0.1%–2.3%) and 0.9% (0.1%–3.9%), respectively. The TOC contents in the core MD22A were relatively high (up to 2.2%) in the interval from 2.5 to 7.5 cmbsf, corresponding to the upper coccolith unit. In the core MD22A, the lower TIC content was in the interval of 10–18 cmbsf. The downcore profiles of the total carbonate contents in the cores MD22A and MD89A showed relatively high trends (Figure 4).

3.4. Correlation coefficient analysis

The Pearson's correlation coefficient, which may indicate the different origins or controlling factors of the trace elements in sediments, e.g., the lithogenous components

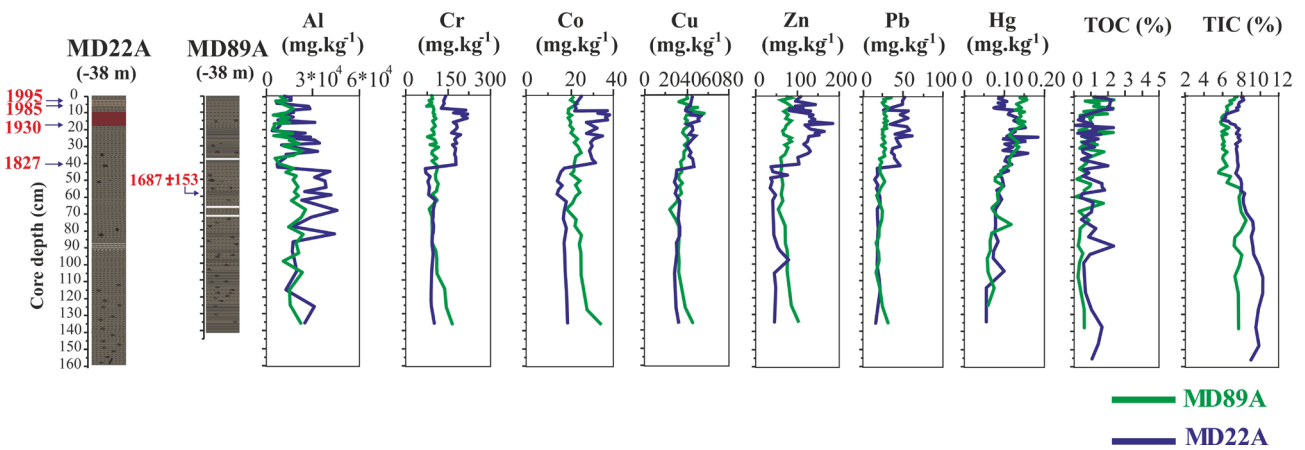

Figure 4. Vertical geochemical profiles (trace element, TOC, and TIC) of cores.

(Rubio et al., 2000), was utilized in the analyses. The correlation coefficients of the trace elements in the Gulf of Gemlik are summarized in Table 3. Significant positive correlations were observed between Al, Cr, Cu, Zn, Co, Pb, and Hg concentrations ($p < 0.01$; Table 3).

3.5. Principal component analysis

According to the results of the PCA, only one PC with Eigen values > 1 was extracted, accounting for a total variance of 77.37% (Table 4). The results indicated significant positive correlations among all studied trace elements. PC1, explaining 77.37% of the total variance, had strong Cu, Co, Pb, Cr, Zn, and Hg factor load values (Table 5).

4. Discussion

4.1. Origin of mass-flow unit and coccolith

The coccolith and mass-flow units were used for correlation between the MD22A and MNTKI-13 cores. The oscillations of gamma density and magnetic susceptibility profiles along the cores showed similarities in the mass-flow units. The cores were correlated using these oscillations. The red-brown mass-flow unit between 22 and 29 cmbsf in the MNTKI-13 core showed physical (magnetic susceptibility) similarities to the similar mass-flow unit between 10 and 18 cmbsf in the MD22A core. However, their stratigraphic location required them to be of different ages. This similarity indicated that the materials of the units were transported from the same sedimentary source. This source was the Kocadere Delta. This was because the presence of similar red sediments was previously detected in the underwater part of the Kocadere Delta in the Gulf of Gemlik (Gasperini et al., 2011). This mass-flow unit was not found in the MD89A core (Figure 2). This result was probably due to the fact that the MD89A core is located in the shallower north-eastern part of the delta, and a mass-flow originating from the delta did not reach this location. Although the low water mass was represented by a counterclockwise current (Figure 1), the circulation was limited in the location of the MD89A core due to the narrow geographic settings. Another important difference between the cores was that the dark grey-brown mud unit overlying the coccolith-laminated unit in the MD22A core was not seen in the MD89A core. The possible reason for this was that MD22A was closer to the sources of pollution (via the Kocasu River); therefore, coccolith production continued.

Table 3. Pearson's correlation coefficient for the trace element concentrations.

	Al	Cr	Co	Cu	Zn	Pb	Hg
Al	1	1.000**	0.983**	0.942**	0.893**	0.716**	0.396**
Cr		1	0.983**	0.942**	0.893**	0.716**	0.396**
Co			1	0.936**	0.864**	0.723**	0.360**
Cu				1	0.858**	0.841**	0.433**
Zn					1	0.736**	0.440**
Pb						1	0.446**
Hg							1

**Correlation is significant at the 0.01 level (2-tailed).

Table 4. Extracted % of variance of principal components analysis.

Component	Initial Eigenvalues			Extraction sums of squared loadings		
	Total	% of variance	Cumulative %	Total	% of variance	Cumulative %
1	4.642	77.372	77.372	4.642	77.372	77.372
2	0.788	13.131	90.504			
3	0.351	5.850	96.353			
4	0.165	2.757	99.110			
5	0.041	0.681	99.792			
6	0.013	0.208	100.000			

Table 5. Component matrix of trace elements.

Trace element	Component
Cu	**0.972**
Cr	**0.961**
Co	**0.951**
Zn	**0.927**
Pb	**0.854**
Hg	0.531

Notes: PCA > 0.6 are shown in bold.
Extraction method: principal component analysis.

4.2. Trace element pollution and its history

This study was conducted using two different core sediment samples from the Gulf of Gemlik, Marmara Sea, Turkey. The vertical trends of the trace elements are shown in Figure 4. The differences observed in terms of accumulation were attributed to ore mineralogy and enrichment processes in different periods (Pan et al., 2011). Assuming that the upper part of the core deposits reflected the industrial period, it can be easier to distinguish the anthropogenic impacts on the sediment. To assess the extent of metal pollution, the background values of study area were calculated using uncontaminated preindustrial sedimentary sections of the cores MD22A and MD89A below 40 cmbsf. The average of the lowest five values of each element with a high ratio of clay (>60%) was used as the background value of the analyzed metals. Based on this assumption, the background values representing the study area were determined in mg kg^{-1} as Al, 27,534.5; Co, 16.7; Cr, 92.5; Cu, 31.7; Pb, 19.4; and Zn, 48.3. In the depth profiles, all selected trace elements were depleted below the 40 cmbsf line in the MD22A. The maximum trace element concentration was observed in the upper layer, where the trace element content was at least 2 times higher than that in the bottom layer, except for the Hg content (Figure 4). The chronology for the upper part (0–40 cmbsf) of the core was based on extrapolation from the mass-flow unit. Based on the radionuclide dates reported by Albut (2014), the lower part of the mass-flow unit could be dated back to 1930. Then, assuming uniform precipitation from the mass flow to the end of the core, the 40 cmbsf level corresponded to about 1827. In the core MD22A, all studied element concentrations started to increase after the year 1827 (corresponding 40 cmbsf, Figure 3). The heavy metal concentrations in the core MD22A were higher than those in MD89A, which may be due to the higher influx of detrital material by mass transport events, which was suggested by the highly fluctuating metal concentrations. In the mass-flow unit, the TOC value dropped to 0.2%–1.0%, which may be due to disrupted water-stratification in the Gulf of Gemlik. The highest concentrations of Cr, Co, Pb, and Zn were found in this unit (10–18 cmbsf interval), corresponding to the sediment deposited in 1930 (Figure 3). The source of this pollution was thought to be the Kocadere Stream. Organic matters of terrestrial origin, as well as pollutants, were transported by Kocasu River. Aykol et al. (2003) reported heavy metal pollution released from Balya Pb–Zn slag and tailing dumps to the Kocasu River. The Balya Pb–Zn Mine District, covers the mine-waste site, the Kocasu River, and Lake Manyas (Budakoğlu and Pratt, 2005). High concentrations of Pb, Zn, and Cd were also reported, and they were compared to average shale and crust in Kocasu River sediments (Budakoğlu and Pratt, 2005). In the core MD22A, the upper coccolith unit was found in the 2.5–7.5 cmbsf interval, corresponding to the sediment deposited during the period from 1995 to 1985. This unit was enriched in TOC (up to 2.2%) but relatively depleted in terms of all studied heavy metals, suggesting dilution by high TIC content (Figure 4). The total inorganic carbon content increased from 40% to 60% in the upper coccolith unit. Coccolith eruptions during this period probably indicate high nutrient input (eutrophication). As a matter of fact, the area contains an artificial silk factory, the Gemlik Fertilizer Factory, and pulp production facilities originating from the olive oil industry, which can cause organic pollution in the region (Albut, 2014). The concentrations of each studied element in the core MD89A was relatively lower than those in the background levels. For this reason, trace element enrichments were not observed in MD89A (Figure 4).

4.3. Assessment of sediment contamination according to EF, I_{geo}, CF, PLI, E_r^i, and RI

High concentrations of trace elements do not always indicate a great degree of pollution (Young et al., 2021; Yüksel et al., 2021). Therefore, in this study, not only was metal distribution examined, but also contamination analysis methods such as EF, I_{geo}, CF, PLI, E_r^i, and RI were used. The EF values calculated for Cr, Co, Cu, Zn, Pb, and Hg in the core sediments (MD22A and MD89A) of the Gulf of Gemlik area are presented in Figure 5. The results of this study showed that the EF value ranges of the studied elements were 0.5–14.6 for Cr, 0.5–14.7 for Co, 0.6–11.1 for Cu, 0.5–27.2 for Zn, 0.5–20.9 for Pb, and 0.9–19.0 for Hg (Table 6). Our results indicated that the MD22A core sediments were enriched (EF > 2) in Cr, Co, Cu, Zn, Pb, and Hg. However, the EF values for these elements were generally lower than 2 for MD89A (Figure 5). The highest EF values were observed in a mass-flow including severely enriched in Cr, Co, Cu, and Hg and very severely enriched in Pb and Zn (Figure 5).

The degrees of heavy metal contamination in the Gulf of Gemlik sediments were also assessed based on the

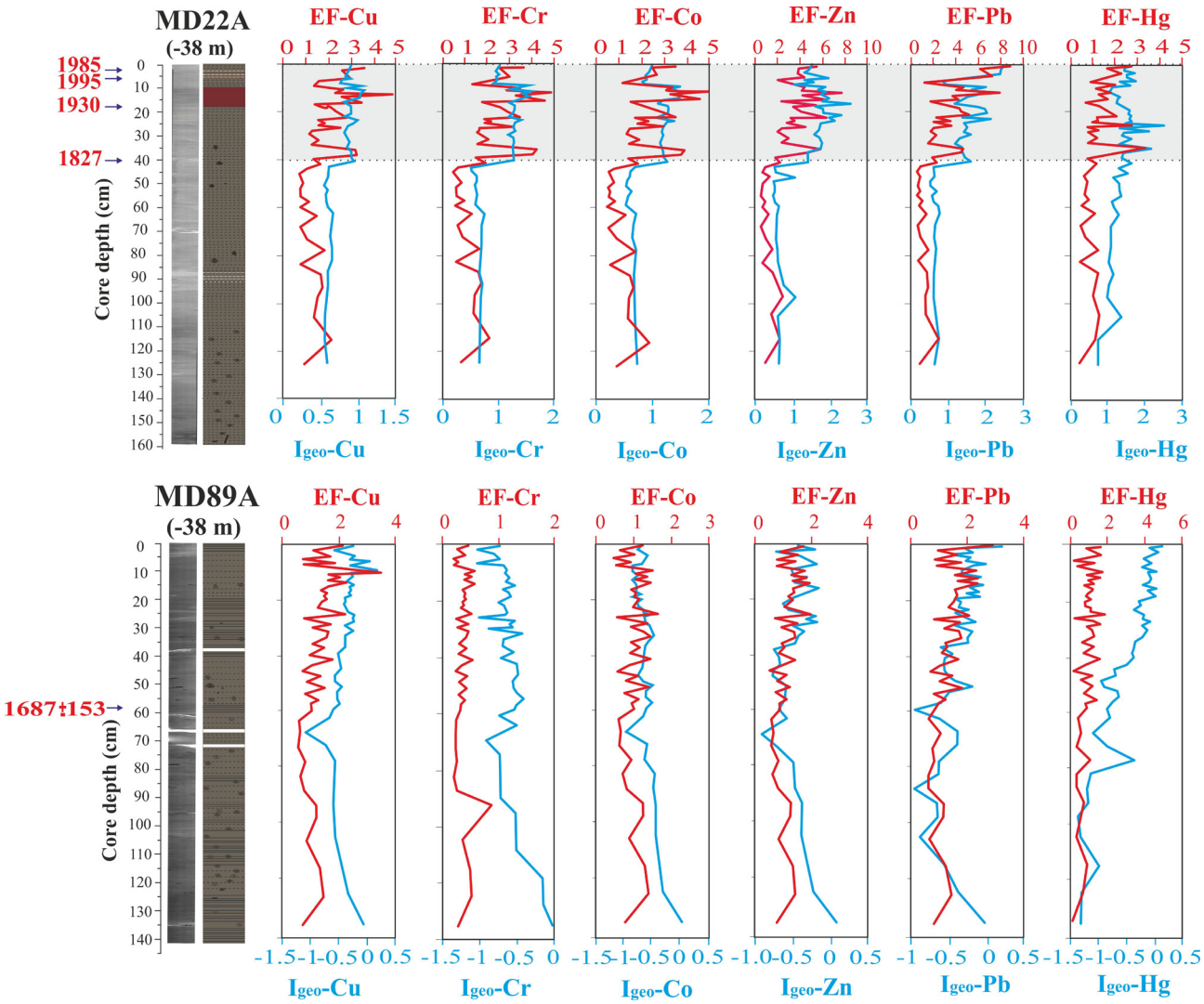

Figure 5. Vertical distribution of enrichment factor (EF) and index of geoaccumulation (I_{geo}) of cores. Grey banded shows high pollution loading of core MD22A.

index of geoaccumulation. The I_{geo} results of the MD22A and MD89A are shown in Figure 5. The I_{geo} mean value for each element in the core MD22A is given in parenthesis; Cr (1.0), Co (1.0), Cu (0.8), Zn (1.3), Pb (1.3), and Hg (1.4). The highest I_{geo} levels were determined at mass-flow. Based on the mean I_{geo} values in this unit, the following order was found: Zn (1.9) > Cr (1.4) > Co (1.3) > Hg (1.2) > Cu (1.0) > Pb (0.3). According to the I_{geo} calculations (Figure 5), the mass-flow unit had Cu contamination degrees varying from uncontaminated to moderately contaminated, and it was moderately contaminated with Pb, Hg, Co, Cr, and Zn. The sediments in MD89A were uncontaminated with Zn, Cr, Co, Hg, Cu, or Pb. The I_{geo} values of all studied elements were low, which indicated no enrichment (values ≤ 0) in the MD89A.

The contamination factor (CF) values were calculated and are given in Table 6. According to the mean CF calculations, the MD22A core sediments were uncontaminated to slightly contaminated with Cr, Co, Cu, and Hg, while they were moderately contaminated with Zn and Pb. However, the CF values for these elements were lower than 2 for MD89A, which indicated that the sediments were uncontaminated to slightly contaminated.

The PLI values were 1.6 for MD22A, and 0.9 for MD89A (Table 6). According to the PLI values, the MD22A core sediments were moderately contaminated with all selected elements, while MD89A was uncontaminated.

The ecological risk statuses of the studied trace elements are shown in Table 6. By calculating the soil ecological risk index, E_r^i, it was found that the risk levels of the MD22A

Table 6. Descriptive statistics of trace elements in core sediments of the Gemlik Gulf.

	MD22A						MD89A					
	Cr	Co	Cu	Zn	Pb	Hg	Cr	Co	Cu	Zn	Pb	Hg
$EF_{minimum}$	0.5	0.5	0.6	0.5	0.5	0.4	0.1	0.4	0.5	0.3	0.5	0.1
$EF_{maximum}$	6.4	6.2	4.6	7.8	9.0	3.4	0.9	1.8	3.7	1.9	3.0	1.9
EF_{mean}	2.1	2.0	1.7	2.8	2.8	1.3	0.3	0.9	1.0	0.8	1.2	0.8
$(I_{geo})_{minimum}$	0.8	0.8	0.6	0.6	0.7	0.9	–1.1	–1.0	–1.1	–0.9	–1.0	–1.4
$(I_{geo})_{maximum}$	1.6	1.5	1.1	2.6	2.5	2.5	0.1	0.0	0.2	0.1	0.2	0.1
$(I_{geo})_{mean}$	0.5	0.5	0.6	0.5	0.5	0.7	–0.6	–0.6	–0.4	–0.5	–0.5	–0.4
$CF_{minimum}$	0.8	0.8	0.9	0.8	0.8	1.1	0.5	0.6	0.5	0.6	0.6	0.4
$CF_{maximum}$	2.4	2.4	1.7	4.1	4.0	3.7	1.4	1.2	1.6	1.4	1.5	1.5
CF_{mean}	1.6	1.5	1.3	2.1	2.1	2.0	0.8	0.8	0.9	0.9	1.0	0.9
$E^i_{r\,minimum}$	1.6	4.1	4.6	0.8	4.1	43.9	1.4	3.8	3.5	0.8	3.8	23.4
$E^i_{r\,maximum}$	4.9	11.9	8.7	4.1	19.8	149.3	3.1	7.7	8.8	1.6	8.6	66.5
$E^i_{r\,mean}$	1.6	1.5	1.3	2.1	2.1	81.5	2.0	4.9	5.7	1.1	5.9	45.9
RI	111.1						55.4					
PLI	1.6						0.9					

and MD89A core sediment samples were low, except for Hg, indicating that the heavy metal pollution in the sediments of the Gulf of Gemlik was relatively light. The range of E_r^{Hg} values was 43.9–149.3, indicating that the Hg in the MD22A core sediments constituted a slightly heavy ecological risk. Similarly, the E_r^{Hg} values ranging from 23.4 to 66.5 indicated that the ecological risk index values of Hg in the MD89A samples were moderate to high. The values of the potential ecological risk index (RI) were 111.1 for MD22A, and 55.4 for MD89A. The main donation of the potential ecological RIs comes from Hg. The input of Hg into the sediments of the study area is of great concern because of the high toxic response factor of this element. The results suggested that the eastern part (MD89A core locations) of the Gulf of Gemlik was characterized by a moderate potential ecological risk, while the southern part was characterized by a high potential ecological risk. This pattern may be due to the fact that the southern part is much more affected by anthropogenic factors than the eastern part (see Section 4.4).

4.4. Pollution sources of trace elements

The PCA results demonstrated that there could be only one main source enriching the trace elements in the MD22A. The mean EF value of all examined trace elements in the upper part (i.e. 40 cmbsf) was greater than 1.5, indicating that trace elements had been affected by anthropogenic factors. The Gulf of Gemlik, especially the localities of Gemlik, Mudanya, and Trilye, are both urbanized industrial areas and resort settlements. The southern coast of the Gulf of Gemlik, where anthropogenic activity levels are high, is much more polluted than the northern coast. The fertilizer industry, iron-steel industry, port activities, fuel tank terminals, and shipping activities constitute the main anthropogenic effects on the Gemlik Gulf sediment (Ünlü et al., 2008). The results of the correlation coefficient revealed strong positive correlations among Cr, Cu, Co, Pb, Zn, and Hg; thus, these metals had been coming from similar sources and originating from similar geochemical processes. Furthermore, the PCA results were correlated well with the Pearson's correlation coefficient values (Table 3). The highest contents of these trace elements were noticed in the 0–40 cmbsf interval, and their content was likely the result of port activities, as well as municipal and industrial effluents. On the other hand, we suggested that not only such anthropogenic activities but also the Kocasu River in the south were the major terrestrial inputs in the Gulf of Gemlik. Clay content in marine sediments is important due to the absorption of high amounts of the trace elements at the surface. Although the two cores from the Gulf of Gemlik had high clay contents, only the MD22A core sediments were polluted with Cr, Co, Cu, Pb, Hg, and Zn according to the EF results. This was because the MD22A core's location was closer to the Kocasu River than the other core. The Kocasu River consists of many tributaries, especially the Nilüfer branch, which drains the domestic and industrial wastewater of Bursa and pollutes the southern shelf area of the Marmara Sea (Sarı, 2008). There are large industrial areas in Bursa, where leather, textile, metal, rubber, and plastic constitute the main products of the industrial sector.

Table 7. Selective trace element content of the Gemlik Gulf core sediments and its correlation with other studies. The concentration units are mg kg^{-1} dry weight.

Site	Al	Cr	Co	Cu	Zn	Pb	Hg	References
$MD22A_{mean}$	20605	139.7	24.4	40	95.2	37.3	0.1	This study
$MD89A_{mean}$	19804	99.1	21.2	37.4	71.2	24.8	0.1	
Ambarlı port	52251	98	X	54	145	29	X	Sarı et al., 2014
Erdek Gulf	26487	111.7	3.9	15.9	26.4	68.4	0.3	Arslan Kaya et al., 2020
Bandırma Gulf	42800	64.2	X	8.9	38.7	27.8	0.9	Mulayim et al., 2012
Northern coast of Marmara Sea	X	47.7	8.6	20.1	42.8	25.4	X	Topçuoğlu et al., 2004
Thermaikos Gulf	X	47	X	80	184	77	X	Christophoridis et al., 2009
Persian Gulf	X	16.1	2.2	15.4	21.1	3.4	0.1	Delshab et al., 2017
Average shale	80000	90	19	45	95	20	X	Turekian and Wedepohl, 1961
Average shale	92000	100	20	57	80	20	0.4	Krauskoph, 1979
Mean sediment	X	72	X	33	95	19	X	Mason, 1966

Notes: X: not analyzed in study.

4.5. Evaluation trace element content by other studies

The trace element contents of the core samples from the Gulf of Gemlik were compared to trace elements data reported for other marine environment sediment studies (Table 7). Table 7 shows that the mean contents of all selected trace elements were relatively high in the sediments of MD22A in comparison to other studies. The mean concentrations of Cr, and Co in the MD22A were higher than those in all other studies that were reviewed for comparisons. Furthermore, the mean Zn sediment concentration in the MD22A core was higher than those at other locations, except for the Ambarlı Port (Sarı et al., 2014) and the Thermaikos Gulf (Christophoridis et al., 2009). The results showed that the mean the Cr and Co concentrations were relatively high, while the mean Cu, Zn, and Pb concentrations were low in the MD22A and MD89A core samples analyzed in this study. The mean Cu content of the MD22A sample in this study was lower than reported from the Ambarlı Port (Turkey), Thermaikos Gulf, and average shale (Turekian and Wedepohl, 1961; Krauskoph, 1979). The mean Hg content in the core sediment from the Gulf of Gemlik in this study was 0.1 mg kg^{-1}. This value showed that the Hg concentration in this study was lower than those reported from the Erdek Gulf (Arslan Kaya et al., 2020), Bandırma Gulf (Mulayim et al., 2012), and average shale (Krauskoph, 1979), except for the Persian Gulf (Delshab et al., 2017), which had an equal Hg value.

5. Conclusions

In this study, two sediment cores were used to reveal pollution loads and history, and sediment quality in the Gulf of Gemlik. Accumulation levels of trace elements, especially heavy metals, were determined through the core sediments with this study. For this purpose, physical properties (gamma density, magnetic susceptibility, grain size) and geochemical properties (trace element, THg, TOC and TIC) of the core sediments were analyzed. The MD22A core included a mass-flow unit and two coccolith units. The upper coccolith unit was deposited between 1995 and 1985, while the mass-flow unit was deposited after 1930. The sedimentation rate for MD22A, excluding the mass-flow unit, was 4.6 cm/year. The concentration of Cr, Co, Cu, Pb, Zn, and Hg in the core MD22A showed marked increases, starting mainly in the 1820s. This pollution was associated with the large amounts of pollutant inputs by anthropogenic activities, especially via the Kocasu River. However, in the core MD89A, there was no enrichment for any of the studied elements.

The long-term monitoring of trace element concentrations in different parts of the Gulf of Gemlik is recommended. Thus, it will be possible to determine the levels of negative and/or ineffective effects of these elements on biota. Such monitoring can also help researchers classify heavy metal sources, such as anthropogenic or natural sources. For this reason, it is important to determine heavy metal levels in the sediment at regular intervals.

Conflict of interest

The authors report no conflicts of interest.

Acknowledgment

The chemicals used in this study were financially supported by the Scientific Research Projects Coordination Unit of İstanbul University. Project number: FBA - 2018 - 29524. We thank the two reviewers and the editor for comments and suggestions that improved the manuscript.

We would like to acknowledge Assoc. Prof. Dr. Denizhan Vardar for his help with the Bathymetry map of Erdek Bay (Fig. 1b).

References

Ackerman F (1980). A procedure for correcting the grain size effect in heavy metal analyses of estuarine and coastal sediments. Environmental Technology Letters 1: 518–527.

Albut G (2014). Heavy metal and organic pollution and its temporal evolution in sediments of Gemlik Gulf. Master Thesis, Istanbul Technical University, Istanbul, Turkey.

Algan O, Balkis N, Cagatay MN, Sari E (2004). The sources of metal contents in the shelf sediments from the Marmara Sea, Turkey. Environmental Geology 46: 932–950.

Arslan Kaya TN, Sarı E, Kurt MA, Acar D (2020). Distribution of Heavy Metal and Enrichment Degree in Core Sediment from Erdek Gulf. Geological Bulletin of Turkey 63: 17-28.

Aykol A, Budakoğlu M, Kumral M, Turan M, Gultekin AH et al. (2003). Heavy metal pollution and acid drainage from the abandoned Balya Pb–Zn Mine. Environmental Geology 45 (2): 198–208.

Bakak Ö, Küçüksezgin F, Özel FE (2020). Assessment of element concentrations in surface sediment samples from Sığacık Bay (eastern Aegean). Turkish Journal of Earth Sciences 29: 1154-1166.

Balcı M, Balkıs M (2017). Assessment of phytoplankton and environmental variables for water quality and trophic state classification in the Gemlik Gulf, Marmara Sea (Turkey). Marine Pollution Bulletin 115: 172-189.

Balls PW, Hull S, Miller BS, Pirie JM, Proctor W (1997). Trace Metal in Scottish Estuarine and Coastal Sediments. Marine Pollution Bulletin 34: 42–50.

Barka AA and Kadinsky Cade K (1988). Strike slip fault geometry in Turkey and its influence on earthquake activity. Tectonics 7: 663–684.

Barka AA and Kuşcu İ (1996). Extends of the North Anatolian fault in the İzmit, Gemlik and Bandırma Bays. Turkish Journal Marine Sciences 2: 93-106.

Beşiktepe S, Sur Hİ, Özsoy E, Latif MA, Oğuz T et al. (1994). Circulation and hydrography of the Marmara Sea. Progress in Oceanography 34: 285–334.

Bhuiyan MAH, Parvez L, Islam MA, Dampare SB, Suzuki S (2010). Heavy metal pollution of coal mine-affected agricultural soils in the northern part of Bangladesh Journal of Hazardous Materials 173, 384-392.

Budakoğlu M and Pratt LM (2005). Sulfur-isotope distribution and contamination related to the Balya Pb–Zn in Turkey. Environmental Geology 47: 773-781.

Christophoridis C, Dedepsidis D, Fytianos K (2009). Occurrence and distribution of selected heavy metals in the surface sediments of Thermaikos Gulf, N. Greece. Assessment using pollution indicators. Journal of Hazardous Materials 15: 1082–1091.

Cüce H, Kalipci E, Ustaoğlu F, Dereli MA, Türkmen A (2022). Integrated spatial distribution and multivariate statistical analysis for assessment of ecotoxicological and health risks of sediment metal contamination, Ömerli Dam (Istanbul, Turkey). Water, Air, and Soil Pollution, 233 (6): 1-21.

Çağatay MN, Wulf S, Sancar Ü, Özmaral A, Vidal L et al. (2015). The tephra record from the Sea of Marmara for the last ca. 70 ka and its palaeoceanographic implications. Marine Geology 361: 96-110.

Delshab H, Farshchi P, Keshavarzi B (2017). Geochemical distribution, fractionation and contamination assessment of heavy metals in marine sediments of the Asaluyeh port, Persian Gulf. Marine Pollution Bulletin 115 (1–2): 401-411.

Duman M, Küçüksezgin F, Eronat AH, Talas E, İlhan T et al. (2022). Combining single and complex indices of pollution with grain size trend analysis of surficial sediments in Edremit Gulf, western Turkey.

Ergin M, Bodur MN, Ediger V (1991). Distribution of surficial shelf sediments in the northeastern and southwestern parts of the Sea of Marmara: strait and canyon regimes of the Dardanelles and Bosporus. Marine Geology 96: 313-340.

Gasperini L, Polonia A, Çağatay MN, Bortoluzzi G, Ferrante V (2011). Geological slip rates along the North Anatolian Fault in the Marmara region Tectonics 30 (6): Article TC6001.

Gaudette H, Flight W, Tanner L, Folger D (1974). An expensive titration method for the determination of organic carbon in recent sediments. Journal of Sedimentary Petrol 44: 249-253.

Hakanson L (1980). An ecological risk index for aquatic pollution control. A sedimentological approach. Water Research 14: 975–1001.

Kırcı Elmas E, Algan O, Özkar-Öngen İ, Struck U, Altenbach AV et al. (2008). Palaeoenvironmental Investigation of Sapropelic Sediments from the Marmara Sea: A Biostratigraphic Approach to Palaeoceanographic History during the Last Glacial-Holocene. Turkish Journal of Earth Sciences 17: 129-168.

Krauskopf KB (1979). Distribution of the elements. In: Krauskopf KB, Emery KO, Legget RF, Murray B, Sloss L (editors). Introduction to Geochemistry, 2nd ed. New York, USA: McGraw-Hill International series in the Earth and Planetary Sciences, pp. 464-487.

Kazancı N, Emre Ö, Erkal T, Görür N, Ergin M et al. (1997). Güney Marmara Deltaları: Kocasu ve Gönen Çayı Deltalarının Morfolojisi ve Tortul Yapısı. Güney Marmara Bölgesinin Neojen ve Kuvaterner Evrimi, YDABÇAG 426/G, Ankara (in Turkish).

Kazancı N, Emre Ö, Erkal T, İleri Ö, Ergin M et al. (1999). Kocasu ve Gönen Çayı Deltalarının (Marmara Denizi Güney Kıyıları) Güncel Morfolojileri ve Tortul Fasiyesleri. MTA Dergisi 121: 33-50.

Kükrer S, Çakır Ç, Kaya H, Erginal AE (2019). Historical record of metals in Lake Küçükçekmece and Lake Terkos (Istanbul, Turkey) based on anthropogenic impacts and ecological risk assessment. Environ. Forensics (in Turkish).

Loring DH (1990). Lithium-a new approach for the granulometrical normalization of trace metal data. Marine Chemistry 29: 156–168.

Loring DH and Rantala RTT (1992). Manual for the geochemical analyses of marine sediments and suspended particulate matter. Earth-Sciences Review 32: 235–283.

Makaroğlu Ö (2021). A Holocene paleomagnetic record from Küçükçekmece Lagoon, NW Turkey. Turkish Journal of Earth Sciences 45: 639-652

Marziali L, Valsecchi L, Schiavon A, Mastroianni D, Vigano L (2021). Vertical profiles of trace elements in a sediment core from the Lambro River (northern Italy): Historical trends and pollutant transport to the Adriatic Sea. Science of the Total Environment 782: 146766.

Mason BJ (1996). Introduction to Geochemistry, 3rd ed. New York, NY, USA: John Wiley.

Mulayim A, Balkis N, Balkis H, Aksu A (2012). Distributions of total metals in the surface sediments of the Bandirma and Erdek Gulfs, Marmara Sea, Turkey. Toxicological & Environmental Chemistry 94 (1): 56–69.

Muller G (1969). Index of geo-accumulation in sediments of the Rhine River. GeoJournal 2: 108–18.

Özkan EY, Fural Ş, Kükrer S, Büyükışı HB (2022). Seasonal and spatial variations of ecological risk from potential toxic elements in the southern littoral zone of İzmir Inner Gulf, Turkey. Environmental Science and Pollution Research.

Özşahin, E (2015). Examination of Gönen and Kocasu River Deltas in terms of land use and changes in shoreline (NW Turkey). International Journal of Innovative Environmental Studies Research 3 (1): 1-13.

Pan K, Lee OO, Qian PY, Wang WX (2011). Sponges and sediments as monitoring tools of metal contamination in the eastern coast of the Red Sea, Saudi Arabia. Marine Pollution Bulletin 62 (5): 1140.

Pekey H (2006). The distribution and sources of heavy metals in İzmit Bay surface sediments affected by a polluted stream. Mar Pollut Bull 52, 1197-1208.

Rani S, Ahmed MK, Xiongzhi X, Keliang C, Islam MS et al. (2021). Occurrence, spatial distribution and ecological risk assessment of trace elements in surface sediments of rivers and coastal areas of the east coast of Bangladesh, North-East Bay of Bengal. Science of the Total Environment 801: 149782.

Reimer PJ, Bard E, Bayliss A, Beck JW, Blackwell PG et al. (2013). IntCal13 and Marine13 radiocarbon age calibration curves 0-50,000 years cal BP. Radiocarbon 55: 1869–1887.

Rubio B, Nombela MA, Vilas F (2000). Geochemistry of major and trace elements in sediments of the Ria de Vigo (NW Spain): an assessment of metal contamination Marine Pollution Bulletin 40: 968-980.

Sarı E (2008). Sources and distribution of heavy metals in river sediments from the Southern Drainage basin of the Sea of Marmara, Turkey, Fresenius Environmental Bulletin 17 (12a): 2007–2019.

Sarı E, Ünlü S, Balcı N, Apak R, Kurt MA et al. (2013). Evaluation of Contamination by Selected Elements in a Turkish Port. Polish Journal of Environmental Studies 22 (3): 841-847.

Sarı E, Ünlü S, Apak R, Balci N, Koldemir B (2014). Distribution and contamination of heavy metals in the surface sediments of ambarlı port area (Istanbul, Turkey). Ekoloji 23: 1-9.

Sarı E, Çağatay MN, Acar D, Belivermiş M, Kılıç Ö et al. (2018). Geochronology and sources of heavy metal pollution in sediments of Istanbul Strait (Bosporus) outlet area, SW Black Sea, Turkey. Chemosphere 205: 387-395

Sarı E, Gümüş U, Çağatay MN, Kurt MA, Kılıç Ö et al. (2020). Distribution and Environmental Risk Evaluation of Metals in Sediment Cores from Marmara Ereğlisi Shelf, Marmara Sea, Turkey. Arabian Journal for Science and Engineering 45: 261-273.

Selvaraj K, Ram Mohan V, Szefer P (2004). Evaluation of metal contamination in coastal sediments of the Bay of Bengal, India: geochemical and statistical approaches. Marine Pollution Bulletin 49: 174–185.

Siani G, Paterne M, Arnold M, Bard E, Metivier B et al. (2000). Radiocarbon reservoir ages in the Mediterranean Sea and Black Sea Radiocarbon 42: 271-280.

Singh H, Pandey R, Singh SK, Shukla DN (2017). Assessment of heavy metal contamination in the sediment of the River Ghaghara, a major tributary of the River Ganga in Northern India. Applied Water Science 7 (7): 4133–4149.

Sohrabi T, Ismail A, Nabavi MB (2010). Distribution and normalization of some metals in surface sediments from South Caspian Sea. Bulletin of Environmental Contamination and Toxicology 85: 502–508.

Sutherland RA (2000). Bed sediment-associated trace metals in an urban stream, Oahu, Hawaii. Environmental Geology 39 (6): 611–627.

Taviani M, Angeletti L, Çağatay MN, Gasperini L, Polonia A et al. (2014). Sedimentary and faunal signatures of the post-glacial marine drowning of the Pontocaspian Gemlik "lake" (Sea of Marmara). Quaternary International 345: 11–17.

Tomlinson DC, Wilson DJ, Harris CR, Jeffrey DW (1980). Problem in assessment of heavy metals in estuaries and the formation of pollution index Helgol. Wiss. Meeresunlter 33 (1980): 566-575.

Topçuoğlu S, Kirbasoglu C, Yilmaz YZ (2004). Heavy metal levels in biota and sediments in the Northern coast of the Marmara Sea. Environmental Monitoring and Assessment 96: 183–189.

Tume P, Bech J, Reverter F, Bech J, Longan L et al. (2011). Concentration and distribution of twelve metals in Central Catalonia surface soils. Journal of Geochemical Exploration 109: 92-103.

Turekian KK and Wedepohl DH (1961). Distribution of the elements in some major units of the earth's crust. Bulletin Geological Society of America 72: 175–192.

U.S. Environmental Protection Agency (1986). Guidelines for health risk assessment of chemical mixtures. Federal Register 51: 34014– 34025.

Usese A, Lucian OC, Rahman MM, Naidu R, Islam S et al. (2017). Enrichment, contamination and geo-accumulation factors for assessing arsenic contamination in sediment of a Tropical Open Lagoon, Southwest Nigeria. Environ Technol Innovat 126-131.

Ünlü S, Alpar B, Aydın S, Akbulak C, Balkıs N et al. (2006). Anthropogenic pollution in sediments from the Gulf of Gemlik (Marmara Sea, Turkey); cause–result relationship. FEB 15 (12a): 1521–1560.

Ünlü S, Topcuoglu S, Alpar B, Kirbasoglu C, Yilmaz YZ (2008). Heavy metal pollution in surface sediment and mussel samples in the Gulf of Gemlik Environmental Monitoring and Assessment 144: 169-178.

Vardar D, Öztürk K, Yaltırak C, Alpar B, Tur H (2014). Late Pleistocene–Holocene evolution of the southern Marmara shelf and sub-basins: middle strand of the North Anatolian fault, southern Marmara Sea, Turkey. Marine Geophysical Research 35: 69–85.

Varol M, Canpolat Ö, Eriş KK, Çağlar M (2020). Trace metals in core sediments from a deep lake in eastern Turkey: vertical concentration profiles, eco-environmental risks and possible sources. Ecotoxicology and Environmental Safety 189, Article 110060.

Varol M, Ustaoğlu F, Tokatlı C (2022). Ecological risks and controlling factors of trace elements in sediments of dam lakes in the Black Sea Region (Turkey). Environmental Research 205 (2022), Article 112478.

Vrhovnik P, Šmuc NR, Dolenec T, Serafimovski T, Dolenec M (2013). Impact of Pb-Zn mining activity on surficial sediments of Lake Kalimanci (FYR Macedonia). Turkish Journal of Earth Sciences 22: 996-1009.

Yaltırak C and Alpar B (2002). Kinematics and evolution of the northern branch of the North Anatolian Fault (Ganos Fault) between the Sea of Marmara and the Gulf of Saros. Marine Geology 190 (1-2): 351–366.

Yaltırak C, Yalçın T, Bozkurtoğlu E, Yüce E (2005). Water-Level Changes in Shallow Wells Before and After the 1999 İzmit and Düzce Earthquakes and Comparison with Long-Term Water-Level Observations (1999–2004), NW Turkey. Turkish Journal of Earth Sciences 14: 281-309.

Yang ZP, Lu WX, Long YQ, Bao XH, Yang QC (2011). Assessment of heavy metals contamination in urban topsoil from Changchun City, China. Journal of Geochemical Exploration 108: 27-38.

Young G, Chen Y, Yang M (2021). Concentrations, distribution, and risk assessment of heavy metals in the iron tailings of Yeshan National Mine Park in Nanjing, China. Chemosphere 271: 129546.

Yu Z, Liu E, Lin Q, Zhang E, Yang F et al. (2021). Comprehensive assessment of heavy metal pollution and ecological risk in lake sediment by combining total concentration and chemical partitioning. Environmental Pollution 269: 116–212.

Yüksel B, Ustaoğlu F, Tokatli C, Islam MS (2021). Ecotoxicological risk assessment for sediments of Çavuşlu stream in Giresun, Turkey: association between garbage disposal facility and metallic accumulation. Environmental Science and Pollution Research (2021), 10.1007/s11356-021-17023-2.

Zhang C, Yu ZG, Zeng GM, Jiang M, Yang ZZ et al. (2014). Effects of sediment geochemical properties on heavy metal bioavailability. Environment International 73: 270–281.

Zhang J, Li X, Guo L, Deng Z, Wang D et al. (2021). Assessment of heavy metal pollution and water quality characteristics of the reservoir control reaches in the middle Han River, China. Science of the Total Environment 799: 149472.